Review article

Taylor Fryett, Alan Zhan and Arka Majumdar*

Cavity nonlinear optics with layered materials

https://doi.org/10.1515/nanoph-2017-0069
Received July 4, 2017; revised August 16, 2017; accepted August 19, 2017

Abstract: Unprecedented material compatibility and ease of integration, in addition to the unique and diverse optoelectronic properties of layered materials, have generated significant interest in their utilization in nanophotonic devices. While initial nanophotonic experiments with layered materials primarily focused on light sources, modulators, and detectors, recent efforts have included nonlinear optical devices. In this paper, we review the current state of cavity-enhanced nonlinear optics with layered materials. Along with conventional nonlinear optics related to harmonic generation, we report on emerging directions of nonlinear optics, where layered materials can potentially play a significant role.

Keywords: exciton-polariton; layered materials; nonlinear optics; optical resonators.

1 Introduction

Layered materials have recently emerged as a promising class of materials for optoelectronics [1]. These materials possess different band gaps leading to a large range of conductivities and the ability to emit and detect light at different wavelength ranges [1]. For example, graphene has no band gap and behaves like a metal; semiconducting transition metal dichalcogenides (TMDCs), such as WS_2, MoS_2, $MoSe_2$ and WSe_2, and black phosphorous have band gaps on the order of 1–2.5 eV, and with its very wide band gap (~6 eV) hexagonal boron nitride (h-BN) is an excellent insulator. Going beyond usual conductivity, exotic properties like superconductivity (TaS_2, $NbSe_2$) [2, 3], ferroelectricity ($CuInP_2S_6$) [4], and ferromagnetism ($Cr_2Ge_2Te_6$, CrI_3) [5–7] have been recently reported in these atomically thin materials. Figure 1A and B show the schematic of the atomic structure for a typical TMDC and graphene. While the bulk of the research in these materials has focused on material characterization, optical spectroscopy and electrical transport measurements, integration of these materials with nanophotonic and nanoelectronic devices is gaining attention. Such integration efforts are primarily motivated by the ease of transferring these extremely thin materials on any substrate without needing explicit lattice matching. Unlike many other quantum confined structures, such as III-V quantum wells or self-assembled quantum dots, these materials stick to the substrate via van der Waals force, and do not require expensive molecular beam epitaxy processes, or wafer bonding. This provides a unique opportunity to develop hybrid photonic platforms where the fabrication processes of the active and passive devices can be completely decoupled. Large-scale, passive photonic integrated circuits will be fabricated using existing foundry systems [9], and subsequently layered materials will be transferred on the pre-fabricated photonic chip to build the active devices, including modulators, detectors, light sources (lasers or light-emitting diodes) and nonlinear optical switches.

Over the last decade, the growth and extensive characterization of these materials have revealed their potential for various electronic and optoelectronic applications. Graphene, inarguably the most studied layered material [10], has found applications in building transistors [11], radio-frequency devices [12], and electronic sensors [13]. In the optoelectronics community, the large electro-optic tunability [14, 15] and strong photo-absorption [16] of graphene generated great interest. However, the extreme thinness of the material, the source of the unusual properties and unprecedented material compatibility of these layered materials also limits the effective light-matter interaction for optoelectronic device applications. To solve this problem, optical device engineers have used various nanophotonic devices integrated with graphene to enhance the light-matter interaction. For example, using nanophotonic waveguides integrated with graphene, the effective light-matter interaction can be increased to build an electro-optic modulator [17, 18], or a photo-detector

***Corresponding author: Arka Majumdar,** Electrical Engineering, University of Washington, Seattle, WA-98195, USA; and Physics Department, University of Washington, Seattle, WA-98195, USA, e-mail: arka@uw.edu
Taylor Fryett: Electrical Engineering, University of Washington, Seattle, WA-98195, USA
Alan Zhan: Physics Department, University of Washington, Seattle, WA-98195, USA

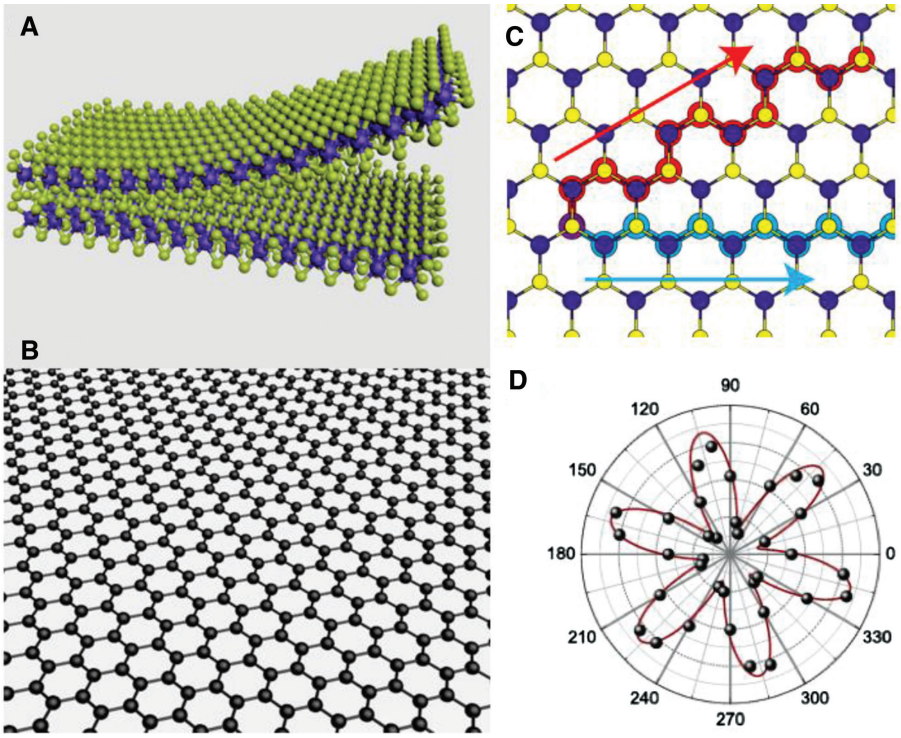

Figure 1: Atomic structure of layered 2D materials.
Crystal structures and SHG spectroscopy of common layered materials. Schematic of (A) layered transition metal dichalcogenide (TMDC) material and (B) graphene. (C) The hexagonal crystal structure of TMDCs. The two directions shown are the zig-zag (show in blue) and arm-chair (shown in red) directions. (D) Due to the six-fold symmetry in the crystal structure, a six-fold pattern is observed in polarization resolved second harmonic generation experiment. Thus, based on the second harmonic signal, crystal axes can be mapped out. Figure 1D is reprinted from Ref. [8].

with high efficiency [19–21]. Further light-matter enhancement and reduction in the size of the device is possible using optical resonators, including photonic crystals [22, 23], ring resonators [18] and plasmonic resonators [24–26]. Optical resonators enhance the light-matter interaction by confining the light both temporally and spatially. For a cavity, the extents of the temporal and spatial confinement are quantitatively given by the quality factor (Q) and mode volume (V), respectively [27]. This trend of integrating graphene with nanophotonic devices continued with TMDCs [28–30]. Cavity integrated TMDCs have been used to demonstrate optically pumped lasing [31–33], cavity-enhanced electroluminescence [34] and strongly coupled exciton-polaritons [35, 36]. In all these devices, the enhancement due to the cavity depends on the Purcell factor $F_p \sim Q/V$ [27, 37].

The success of optical resonators to enhance the light-matter interaction in layered materials motivated researchers to study cavity nonlinear optics using these materials. Due to their bosonic and chargeless nature, the interaction strength between photons is very weak and nonlinear optical effects appear only at very high power. This remains an outstanding challenge to be overcome for optics to be used for any compute applications. However, the required power can be lowered using optical resonators. For a cavity-enhanced second-order $\chi^{(2)}$ (third-order $\chi^{(3)}$) nonlinear switch, the threshold power is proportional to V/Q^3 (V/Q^2) [38]. The ability of nano-cavities to spatially confine light of wavelength λ to an extremely small mode volume [$V \sim (\lambda/n)^3$ where n is the refractive index of the cavity material], and store light for a few nanoseconds ($\tau_{ph} = Q\lambda/2\pi c$) provides an opportunity to realize optical nonlinearity at the few photon level. Thus, cavities can significantly enhance the intrinsic optical nonlinearity of the layered materials. In this paper, we review the recent progress in the field of cavity nonlinear optics with layered materials. We note that the nonlinearity of layered materials is comparable to that achievable of existing material systems, including quantum confined structures and bulk materials. However, the ability to integrate these materials with any material systems provides an excellent opportunity to build hybrid integrated nonlinear photonic systems. Apart from the cavity-enhanced second-order and third-order nonlinear optics, the layered materials

exhibit saturable absorption and nonlinear polariton-polariton interaction. Finally, the layered materials host defect centers, which are essentially two-level systems, and will provide a route to obtain single photon nonlinearity. Along with reviewing the existing works, we will lay out the outstanding challenges and several future directions of the cavity nonlinear optics with these emerging layered material systems.

2 Nonlinear processes in layered materials

In recent years, several experiments with stand-alone layered materials measured their nonlinear optical coefficients. Table 1 summarizes the measured $\chi^{(2)}$ and $\chi^{(3)}$ coefficients for different layered materials. The large $\chi^{(2)}$ values near ~800 nm originate from the energetic proximity of the excitons in TMDCs, and thus generally come with large losses [8, 46–48, 51]. These experiments also clearly showed that the second-order nonlinearity in TMDCs is the strongest at the single layer limit. With an even number of layers, this nonlinearity disappears, as the material becomes centrosymmetric. Thus, the nonlinear signal works as a convenient microscopy tool for probing the number of layers in the TMDC crystal. Additionally, a six-fold polarization pattern is found in the second harmonic signal reflecting the hexagonal crystal structure of the TMDCs (Figure 1C and D). Thus, nonlinear spectroscopy of the layered materials has become an indispensable tool to determine the crystalline orientation, thickness uniformity, layer stacking, and single-crystal domain size of atomically thin films [47, 49, 52, 53]. In fact, this technique is critical for creating the heterostructures of TMDC layers, as the relative crystal orientation determines the heterostructure's electronic band structure [54]. Researchers have also demonstrated that the centrosymmetry of bilayer MoS_2 can be broken with a static electric field, enabling second harmonic generation (SHG) [55]. Note that this electric field-induced SHG can potentially create opportunities for electro-optic switching applications. Another way to break the symmetry will be via straining the bilayers. Straining monolayers and bilayers of MoS_2, researchers have already demonstrated band gap engineering and photoluminescence (PL) control [56–58]. However, strain induced nonlinear optics with layered matierlas have yet to be reported. In addition to experimental measurements, several research groups have reported atomistic simulation studies to estimate the nonlinear coefficients for different layered materials [59–61], and have also analyzed the effect of substrates [62]. This work models the nonlinearity of layered materials as zero-thickness interfaces, and showed that without careful theoretical modelling, the extracted value of the nonlinear coefficient can be largely exaggerated.

Table 1: Reported nonlinear optical coefficients in layered materials: SI unit for $\chi^{(3)}$ -coefficients is m^2/V^2 and for $\chi^{(2)}$ -coefficients is m/V.

Material [Ref]	Type of NLO ($\chi^{(3)}$, $\chi^{(2)}$)	Approx. λ(nm)	Value (SI unit)
Graphene [39]	$\chi^{(3)}$	800	1.4×10^{-15}
Graphene [40]	$\chi^{(3)}$	1550	3.25×10^{-19}
BP [41]	$\chi^{(3)}$	1550	1.4×10^{-19}
MoS_2 [42]	$\chi^{(3)}$	1550	2.9×10^{-19}
GaSe [43]	$\chi^{(3)}$	1550	1.7×10^{-16}
ReS_2 [44]	$\chi^{(3)}$	1550	5.3×10^{-18}
WSe_2 [45]	$\chi^{(2)}$	1550	60×10^{-12}
WS_2 [46]	$\chi^{(2)}$	800	10×10^{-9}
MoS_2 [47]	$\chi^{(2)}$	800	100×10^{-9}
WSe_2 [48]	$\chi^{(2)}$	800	10×10^{-9}
h-BN [49]	$\chi^{(2)}$	800	1×10^{-11}
GaSe [50]	$\chi^{(2)}$	1550	700×10^{-12}

BP, Black phosphorous.

Most studies with TMDCs have focused on pumping near the exciton resonance (~800 nm) and creating a second harmonic above the band gap at ~400 nm. A more interesting regime from an application point of view is to pump near 1550 nm and create a second harmonic signal at 775 nm. This wavelength range is particularly important for interfacing with telecommunication technologies. Such nonlinear devices could be utilized for optical bistability for a telecommunication wavelength laser [63]. In this wavelength range, the absorptive loss at the fundamental frequency is also minimal. Researchers have demonstrated SHG under pump near 1550 nm in stand-alone, monolayer WSe_2 [45] and in GaSe [50]. In WSe_2, researchers also demonstrated electric field controlled SHG showing the nonlinear optical effect far from the excitonic frequency is strongest at twice the exciton frequency. Thus, by changing the exciton frequency, one can change the effective nonlinearity. The reported $\chi^{(2)}$ values for WSe_2 are around 60 pm/V at 1550 nm and for GaSe, the $\chi^{(2)}$ value is estimated to be at least one order of magnitude larger (Table 1).

In addition to second-order nonlinear processes, third-order nonlinear processes have also been studied using layered materials. Being centrosymmetric, graphene does not possess intrinsic second-order nonlinearity, and hence graphene is primarily studied for third-order nonlinear processes. Several research papers explore third harmonic generation [39], cascaded third harmonic

generation [64], and four wave mixing [65]. Layer-dependent third harmonic generation is also recently reported in black phosphorous [41]. In TMDCs, researchers have demonstrated intensity-dependent refractive index by exploiting the third-order nonlinearity [66].

We note that, the measured values of the nonlinear coefficients in infrared wavelengths (~1500 nm) are comparable to the $\chi^{(3)}$ of bulk silicon (~10^{-19} m^2/V^2) or the $\chi^{(2)}$ of bulk III–V materials, such as GaAs or GaP (~100×10^{-12} m/V), as a research article has pointed out in the past [67]. Thus, the utility of nonlinear layered materials does not necessarily originate from a large nonlinearity *per se*, but rather from their tunable optical nonlinearity, their ease of integration onto arbitrary substrates, ease of patterning, and the possibility of creating a hybrid platform. For example, complementary metal-oxide-semiconductor (CMOS)-compatible materials, such as silicon and silicon nitride, lack second-order optical nonlinearity. By integrating layered materials on top of them, we can realize second-order nonlinearity in a CMOS compatible way. Thus, in our opinion, the true benefit of layered materials lies in creating hybrid, active photonic systems.

3 Cavity-enhanced second harmonic generation

While there is significant research progress in the nonlinear optics of layered materials, the extreme thinness of the material poses a serious problem for practical applications. This problem can be ameliorated by using an optical resonator to enhance the effective nonlinearity. While the effective nonlinearity in a layered material clad cavity is proportional to the material nonlinearity, the material interacts only with a small portion of the field on the surface. Hence it is important to estimate the effective nonlinearity in the presence of an optical resonator.

3.1 Modeling of the nonlinear cavity

In a recent work, Majumdar et al. [68] analyzed the effective nonlinearity of a layered material clad nano-cavity for second-order nonlinear optics. They assume that the optical cavity is formed in a dielectric slab with the field profile varying sinusoidally inside the slab, and decaying exponentially outside (Figure 2A). While such a model is a simplification, and neglects the actual mode profiles of the cavity, it allows the authors to obtain a closed form analytical expression, which provides an intuitive understanding of the effective nonlinearity. They find that the nonlinear interaction strength g_{nl} is given by [68]:

$$\hbar g_{nl} \approx \left(\frac{\hbar\omega_o}{2\varepsilon_o}\right)^{3/2} \frac{2\chi^{(2)} dS^3}{3\varepsilon^{3/2}\sqrt{\pi\sigma_x\sigma_y}},$$

where $\hbar$ is the reduced Planck's constant, ω_o is the fundamental angular frequency, $\chi^{(2)}$ is the value of the second-order nonlinear coefficient, d is the thickness of the layered materials, ε is the dielectric constant of the layered material, S signifies the ratio of the field strength at the surface and center of the slab, and σ_x and σ_y are the confinement length of the optical field inside the resonator along x and y directions. Note that, a stronger localization within the nonlinear material will increase the nonlinear

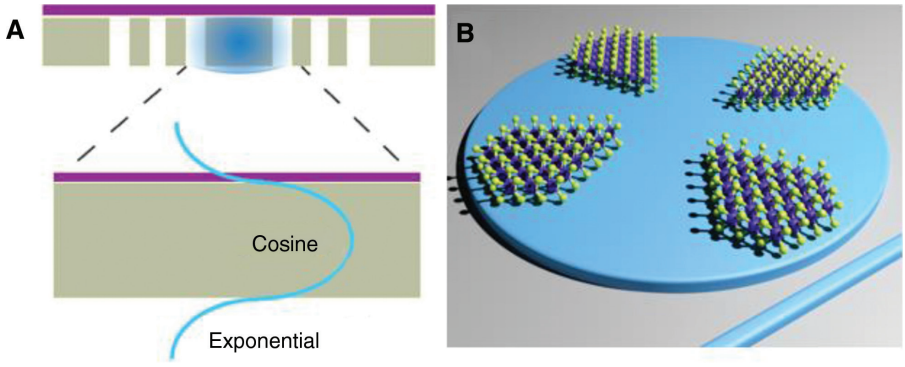

Figure 2: Modeling of nonlinear layered material integrated optical resonator.
(A) The theoretical model to estimate the effective nonlinearity for a layered material placed on top of the cavity assumes the cavity mode follows a cosine function inside the slab, and decays exponentially outside the slab. (B) Schematic of a disk with patterned layered material on top: by intelligently patterning the material on top, the mode profiles are not significantly altered, but the nonlinear overlap can be significantly improved.

interaction strength. A cavity helps to confine light and thus reduces both σ_x and σ_y. They also find that the interaction strength depends on the product of the nonlinear coefficient and the material thickness, as one would expect. Thus, the small thickness of the layered materials indeed limits the interaction strength. However, the analytical expression also shows that by enhancing the field on the surface, i.e. by increasing the value of *S*, the effective nonlinearity can be significantly enhanced. This criterion necessitates rethinking the design of the dielectric optical cavities, where the field is generally minimized on the surface to reduce the loss. In a more recent paper, the authors have also shown that layered materials provide a novel way to satisfy phase-matching condition in second-order nonlinear optics as elaborated below.

In deriving the analytical expression of the nonlinear interaction strength, it was previously assumed that the phase-matching condition is fully satisfied. In second-order nonlinear optics, the phase-matching condition is equivalent to satisfying the momentum conservation of the interacting waves [69]. In a nano-cavity, satisfying this condition amounts to having a good modal overlap between the fundamental and the second harmonic modes. Moreover, for high efficiency, the cavity needs to support modes at both frequencies. Satisfying both of these requirements is difficult, and to date, the proposed designs require stringent fabrication tolerance, and often involve significant computational resources [70]. A single monolayer does not significantly change the confined mode profiles in the cavities as the interaction is evanescent in nature, and due to the extreme thinness of the material, only slightly perturbs the cavity mode. Thus, 2D materials provide an excellent opportunity to decouple the cavity design and nonlinear material design. Starting with any cavity, and intelligently patterning 2D materials on top of it, the phase-matching condition can be satisfied. A schematic of a nano-resonator with patterned 2D material on top is shown in Figure 2B. Our theoretical analysis shows that such patterning can maintain a good overlap integral, and thus retain significant effective nonlinearity, even when the modes are largely mismatched [71].

The model described above primarily works for a dielectric optical resonator, and currently most of the reported results on cavity nonlinear optics with layered materials involve dielectric resonators. However, plasmonic resonators already are being used to enhance the linear properties of the layered materials [72], including light emission [32, 73], electro-optic modulation [25] and photo-detection [74]. Recently, evidence of polariton formation has also been observed in plasmonic cavities [75]. Plasmonic resonators can also be engineered to have multiple resonances [73], and thus can be ideal for second and third harmonic generation. While the quality factors of plasmonic resonances are significantly lower compared to dielectric resonators due to metallic losses, they provide an extremely small mode volume to which significantly enhances the light-matter interaction. Additionally, plasmonic effects can be exploited to confine light to lie in a single plane, where the layered material can be placed. Thus, plasmonic resonators are expected to play an important role in enhancing nonlinear optical effects in layered materials. Another important research direction could be to develop hybrid plasmonic-dielectric resonators to realize both high *Q* as is characteristic of dielectric cavities, with the low *V* that is characteristic of plasmonic cavities.

3.2 Second harmonic generation with single mode cavity

Current experimental efforts on SHG with layered materials are primarily focused on a single cavity mode coupled to exfoliated layered materials. Using a tungsten diselenide (WSe_2) clad silicon photonic crystal cavity, Fryett et al. [76] showed enhanced SHG. In this work they used a pulsed laser operating within the telecommunication band (~1550 nm). Figure 3A shows the scanning electron micrograph of a WSe_2 clad silicon photonic crystal cavity. The cavity modes are near 1490 nm. When the cavity is resonantly excited using a pulsed laser, they observed a strong second harmonic signal around 745 nm (Figure 3B). In the second harmonic signal, they observed a Gaussian background which comes from the doubling of the laser wavelengths, which are off-resonant from the cavity. In this background, they observed a Lorentzian peak at exactly the half-wavelength of the cavity resonance, signifying the cavity-enhanced SHG. The reported enhancement is only ~100, primarily because of the lack of a cavity mode at the second harmonic frequency and low Q-factor of the cavity ($Q \sim 100$). Moreover, silicon absorbs a significant amount of second harmonic signal. A promising solution will be to make a doubly resonant cavity out of wide bandgap materials, such as silicon nitride [30] or silicon dioxide [78]. Researchers also recently demonstrated continuous wave (CW) SHG using GaSe coupled with silicon photonic crystal cavity with a pump laser at ~1550 nm [79]. The required optical power in this work is only microwatts, primarily due to the high Q-factor and small mode-volume of the photonic crystal cavities.

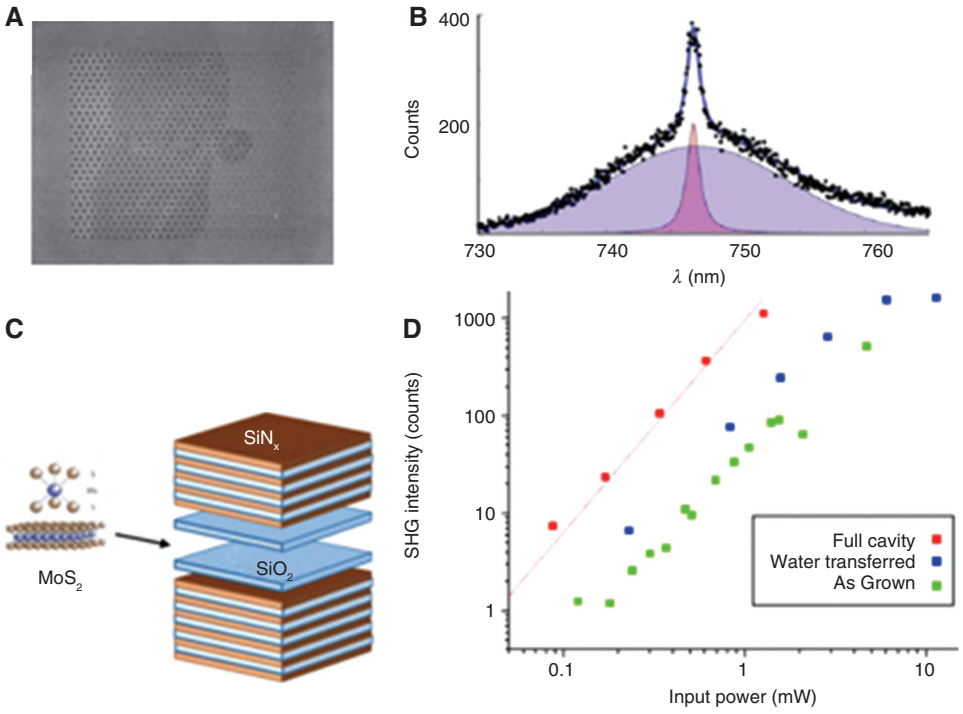

Figure 3: Cavity-enhanced second-order nonlinear optics with layered materials.
(A) Scanning electron micrograph (SEM) of a WSe_2-clad silicon photonic crystal cavity. (B) Measured spectrum of the second harmonic signal shows the Gaussian background with a Lorentzian peak signifying the cavity resonance. (C) Schematic of a distributed Bragg reflector (DBR) cavity with MoS_2 placed in between two mirrors. The DBR is made of alternating layers of silicon dioxide and silicon nitride. (D) The measured intensity of the second harmonic generated light shows a clear enhancement due to the cavity. Figures (A) and (B) are reprinted from Ref. [76]; Figures (C) and (D) are reprinted from Ref. [77].

In another experiment, Day et al. [77] demonstrated SHG using MoS_2 integrated inside a distributed Bragg reflector (DBR) cavity (Figure 3C and D). In this experiment, the DBR is formed by using alternating layers of silicon nitride and silicon dioxide to minimize the absorption of light. Here, the SHG is observed under pulsed excitation at 800 nm. The reported enhancement is ~10. The lower enhancement factor can be attributed to low Q-factor of ~20, and the large mode-volume of the DBR cavity. An open hemiconfocal cavity geometry [80] might be more suitable to reduce the mode volume and thus further enhance the nonlinearity.

3.3 Second harmonic generation with double mode cavity

The enhancement factor can be significantly increased by using cavity modes both at the fundamental and the second harmonic frequency. Such mode engineering is theoretically difficult at the nano-scale, but can be easily realized in a DBR-based Fabry-Perot cavity. However, inevitable fabrication errors prevent the cavity modes from appearing exactly at the desired resonance wavelengths. Yi et al. [81] solved this problem by creating a mechanically tunable Fabry-Perot cavity, where the bottom mirror is a DBR, and the top mirror is a capacitively actuated silver mirror (Figure 4A). The capacitive tuning enables changing the cavity length, and thus cavity resonances. Via mechanical tuning, it is possible to bring both the fundamental and the second harmonic modes to the desired frequencies. In this experiment, they used MoS_2 as the nonlinear material, and despite their low cavity Q-factor, the reported enhancement is ~3000 (Figure 4B and C). This experiment used a pulsed excitation near 930 nm. Further improvement is possible by improving the cavity Q-factor, and reducing the mode-volume, which is often very large in Fabry-Perot cavities.

Phase-matched SHG was also recently reported in a silicon photonic waveguide using $MoSe_2$ [82]. By engineering the waveguide cross-section, the effective mode-indices of the fundamental and second harmonic modes are matched, which ensures the phase-matching of the light at the fundamental and second harmonic frequencies. Similar methods have been used for designing phase-matched ring resonators for cavity nonlinear optics using aluminum

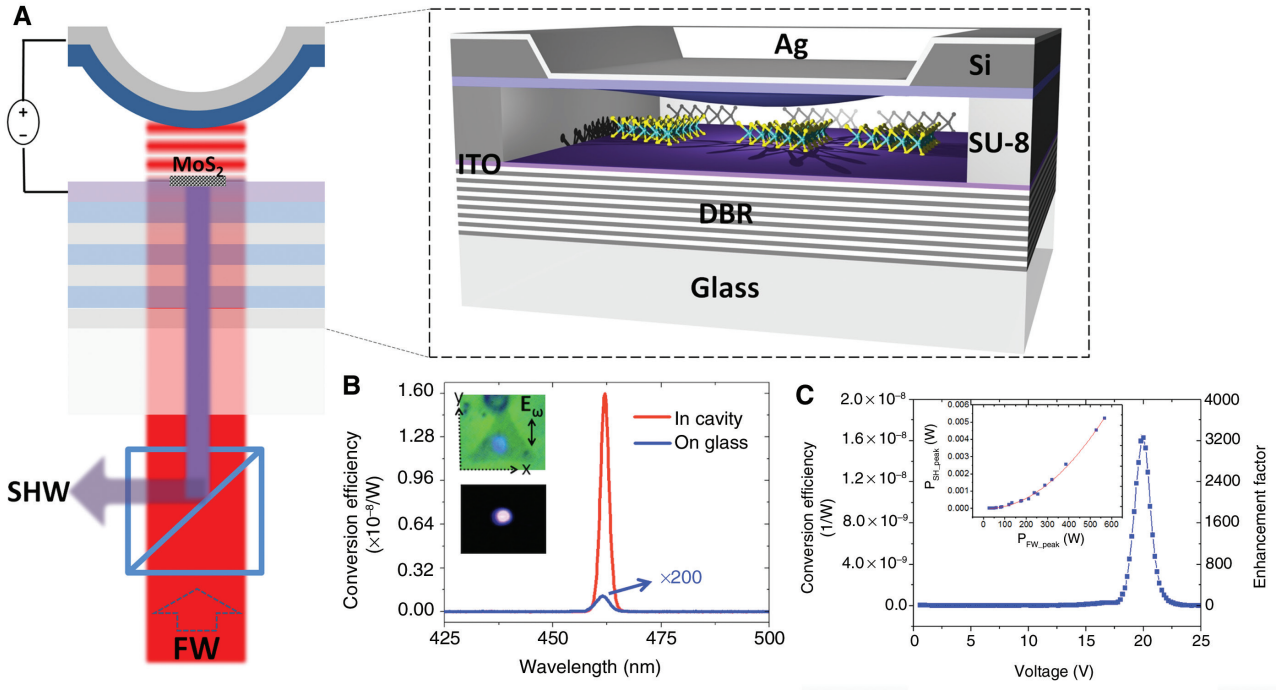

Figure 4: Second harmonic generation in double-mode cavity.
(A) Schematic of the mechanically tunable Fabry-Perot cavity with embedded MoS_2. (B) The frequency conversion efficiency is increased due to the presence of the cavity. (C) By applying the voltage, the cavity modes can be tuned, and a large enhancement can be achieved when the cavity is tuned such that modes appear at the fundamental and harmonic frequencies. Figures are reprinted with permission from Ref. [81]. Copyright (2016) American Chemical Society.

nitride [83]. Such a phase-matched ring integrated with layered materials can enhance the efficiency of the second-order nonlinear processes.

All the existing experiments so far have reported significantly lower SHG efficiency, compared to the theoretical predictions. For a given power, the efficiency can be improved by increasing the quality factor and reducing the mode volume. Another limiting factor might be the transfer of the layered materials, which generally involves organic polymers, and might introduce excess loss coming from the polymer residues. Having the resonances at both the fundamental and the second harmonic frequencies will also increase the efficiency significantly. Along with innovating cavity structures, new layered materials with stronger nonlinear optical properties, such as multiferroics [84], can also improve the overall efficiency of SHG.

4 Third-order nonlinear processes

While most of the recent works on cavity nonlinear optics using layered materials primarily focused on second-order nonlinear optics, the first demonstration of cavity nonlinear optics was with third-order nonlinearity of graphene. Gu et al. [85] demonstrated optical bistability and regenerative oscillation using a graphene-clad silicon photonic crystal cavity. Figure 5A shows the fabricated photonic crystal cavity which is coupled to a waveguide. Graphene is transferred onto the cavity, and under ~1562 nm CW excitation optical bistability is observed (Figure 5B). The threshold power where the bistable behavior appears in graphene-silicon resonator is lower than that observed with a bare silicon photonic crystal cavity.

In the authors' opinion, however, the third-order nonlinearity with 2D materials is not as attractive as second-order nonlinear optics from an application point of view. As most materials already possess strong third-order nonlinearity, and the measured values of nonlinearity for graphene and black phosphorous are almost the same order of magnitude as silicon, the application area of third-order nonlinear optics with layered material is debatable [67]. However, for many applications, requiring high power operation, silicon is not ideal due to high two-photon absorption when operating at the telecommunication wavelength. In those applications, silicon nitride and silicon dioxide are gaining popularity due to their wide

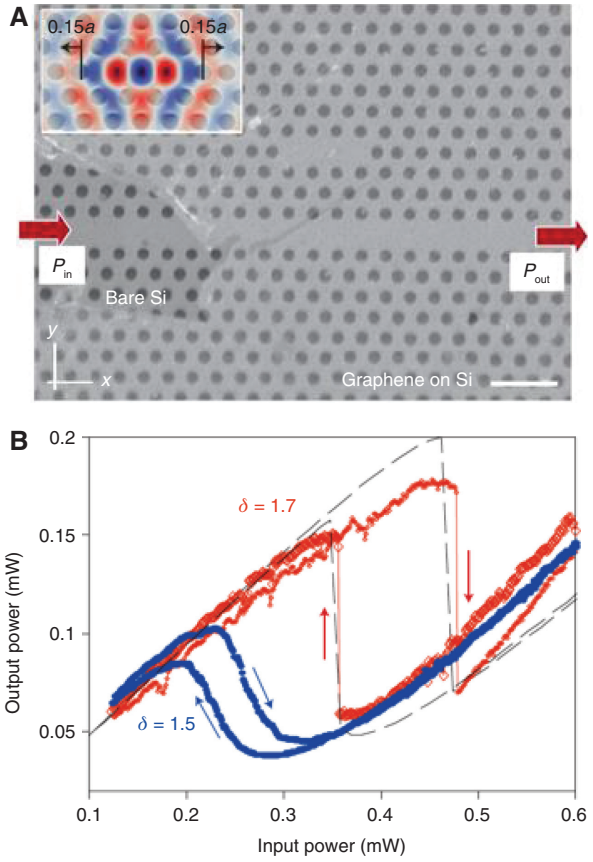

Figure 5: Optical bistability with graphene-clad silicon photonic crystal cavity.
(A) Scanning electron micrograph (SEM) of the graphene-clad photonic crystal cavity; (B) output power as a function of the input power clearly shows the signature of optical bistability. The figures are reprinted from Ref. [85].

band gaps [86]. The magnitude of the third-order nonlinear coefficient in layered materials is higher compared to that of the nitride ($\chi^{(3)} \sim 1\times10^{-20}\ m^2/V^2$) [87] or oxide ($\chi^{(3)} \sim 2.5\times10^{-22}\ m^2/V^2$) [69], and will play an important role in realizing low-power nonlinear optics.

5 Saturable absorption

Another promising nonlinear optical effect in layered materials is their saturable absorption. Due to the extreme thinness of layered materials, their photo-absorption can be easily saturated with low optical power. A common application of saturable absorption is the integration into optical cavities to generate pulsed laser sources, both in fiber and free space systems. Many recent papers on pulsed lasers have utilized layered 2D materials as the saturable absorption material of choice [88–90]. Most of these works used graphene as the saturable absorber. One particularly appealing aspect of graphene is its broadband absorption due to its lack of a band gap, which allows mode-locking over a large wavelength range, including in the mid-infrared wavelengths. Figure 6A shows an experimental setup with a graphene saturable absorption mirror [88]. In this work, stable mode-locked laser pulses as short as 729 fs were obtained with a repetition rate of 98.7 MHz and an average output power of 60.2 mW at ~2 μm (Figure 6B). In addition to the free-space setup, saturable absorption in graphene was used in a fiber laser to demonstrate mode-locking (Figure 6C) [89]. In this work, they created a passively mode-locked erbium-doped fiber laser working at 1559 nm, with 460 fs pulse duration (Figure 6D). Recently, several works reported similar mode-locked laser systems with a variety of atomically thin materials including black phosphorous [91], MoS_2 [92] and WS_2 [93]. Additionally, researchers have used black phosphorous, WS_2 and MoS_2 solutions as saturable absorbers to construct passively Q-switched Nd:YVO_4 lasers, with pulse durations of few nanoseconds [94].

6 Nonlinear exciton-polaritons

So far, most of the nonlinear optical effects we discussed are observed with light sources off-resonant from the exciton. Very near the exciton resonances, a large nonlinearity can be realized using the polaritonic system formed by strong coupling between the cavity-confined photons, and the excitons in the layered materials. Recent works reported observation of strongly coupled exciton-polaritons using layered materials, including MoS_2 and bilayer $MoSe_2$ [35, 36]. Figure 7A shows the schematic of the open DBR cavity used to demonstrate strong coupling between the cavity mode and the exciton [35]. The open cavity architecture allows tuning the cavity resonance by mechanically displacing one of the cavity mirrors. When the cavity mode is tuned across the excitonic resonance, anti-crossing between the cavity mode and the exciton is observed, signifying strong coupling and polariton formation. Figure 7B shows the upper and lower polaritons measured in PL.

Exciton-polaritons using quantum wells have been previously used to extensively study “quantum fluids of light” [95]. At low excitation power, the exciton-polariton system behaves linearly as the exciton-exciton interaction is weak. Bose-Einstein condensation (BEC) of exciton-polaritons has also been observed by several groups [96, 97]. The polaritons have much smaller effective mass compared to atoms due to their photonic components,

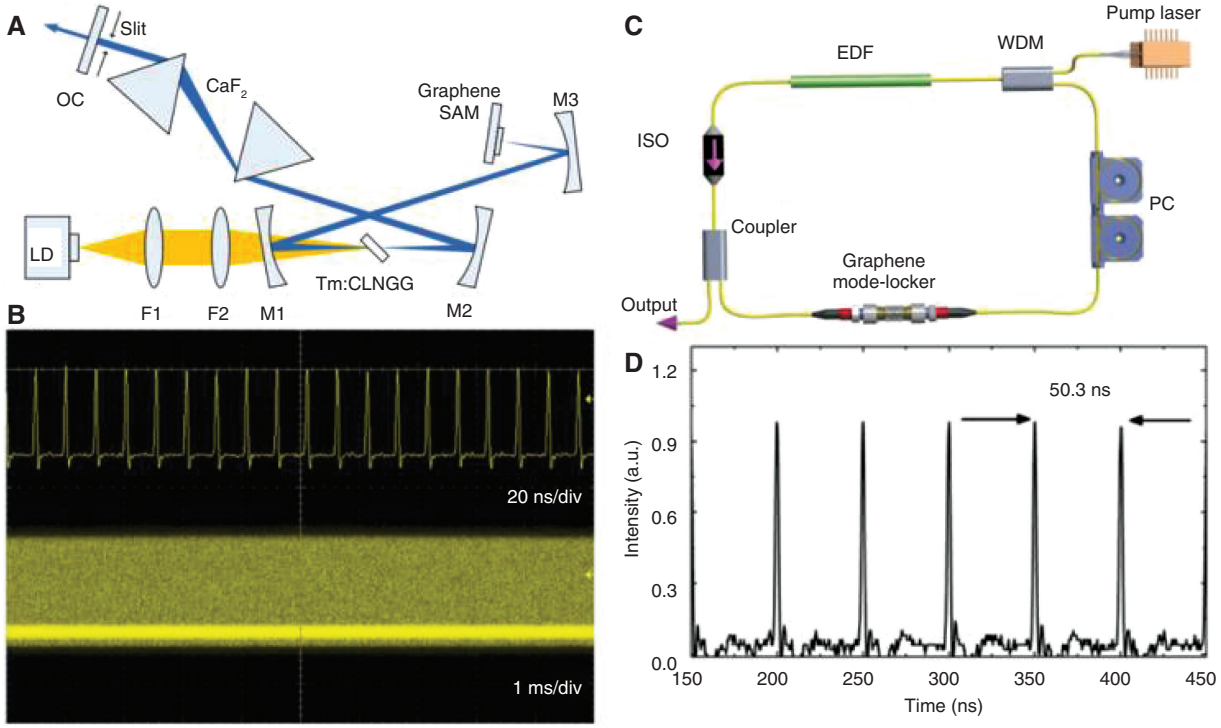

Figure 6: 2D material based mode-locking.
(A) Experimental setup of the mode-locked laser based on the graphene saturable absorption mirror; (B) CW mode-locked pulse trains in nanosecond and millisecond time scales; (C) graphene mode-locked fiber laser where the mode-locker assembly contains a graphene flake. (D) Auto-correlation trace of output pulses showing the pulse repetition rate of 19 MHz. Figures (A) and (B) are reprinted from Ref. [88]. Figures (C) and (D) are reprinted with permission from Ref. [89]. Copyright (2010) American Chemical Society.
EDF, erbium-doped fiber; ISO, isolator; PC, polarization controller; WDM, wavelength division multiplexer.

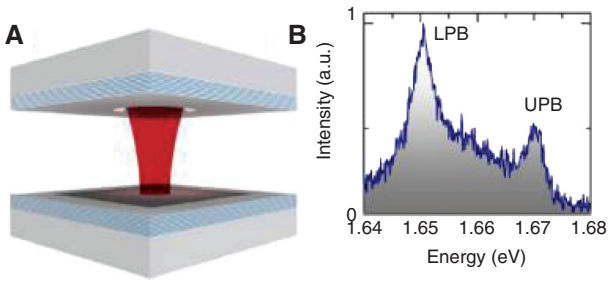

Figure 7: Exciton-polaritons in layered materials.
(A) Schematic of the open distributed Bragg reflector (DBR) cavity with layered material inside the cavity. The top mirror of the cavity can be mechanically displaced to tune the cavity resonance. (B) Photoluminescence spectrum of the strongly coupled exciton-polariton system clearly shows the upper and lower polaritons. The figures are reprinted from Ref. [35].

and thus the BEC can be realized at a much higher temperature. Moreover, the extremely large binding energy (~0.2–0.8 eV) in TMDC excitons can potentially allow creation of polaritons and condensates at room temperature. Such condensation has not yet been observed in layered materials, but is theoretically predicted [98]. Theory also predicts observation of topological polaritons [99] and exciton-mediated superconductivity using the TMDC exciton-polaritons [100]. With higher excitation power, however, one cannot create an arbitrary number of excitons [97]. Thus, the fermionic nature of the constituent electron and hole in the exciton-polariton becomes more prominent in high density exciton-polaritons, and strong polariton-polariton repulsion can be observed. When the exciton density reaches the Mott density, the exciton-polariton system can potentially exhibit BEC-BCS crossover [97]. Thus, layered material based exciton-polaritons and their condensates can potentially provide a strongly nonlinear material platform.

Additionally, the extreme thinness of the layered materials allows for straightforward patterning by etching. Thus, one can easily pattern them to create small islands of layered materials, which should behave like quantum dots (Figure 8A). The size and position of these islands can be easily controlled by lithography [101]. Performance of such quantum dot like structures has been theoretically analyzed [102]. In TMDCs with excitonic

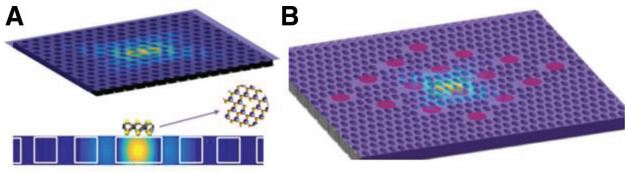

Figure 8: Patterned quantum dots in layered materials.
(A) By patterning layered 2D materials, we can create quantum dot like structures, where the exciton-exciton interaction can be significantly enhanced. (B) These patterned quantum dots can be placed in an array and coupled with an array of interacting optical resonators. Thus, a network of nonlinear nodes can be created.

Bohr radius of only 1 nm, theoretical analysis showed that when the radius of the patterned material reaches a few tens of nm, single photon nonlinear optics can be observed [103]. Specifically, polaritonic blockade can be realized in these quantum dot like structures. The ability to deterministically position these structures via lithography can potentially create an array of interacting single photon nonlinear systems (Figure 8B). Researchers have already designed and fabricated an array of linear cavities [104, 105]. The addition of the single photon nonlinearity in each of these cavities will create a testbed to study non-equilibrium quantum many body physics with correlated photons [106–108].

7 Single photon nonlinear optics

Several theoretical proposals explored the feasibility of reaching single photon nonlinear optics using the second-order and third-order optical nonlinear materials, coupled to optical resonators [109, 110]. As layered materials can be integrated with high-Q silicon or silicon nitride cavities, it is indeed possible to reach single

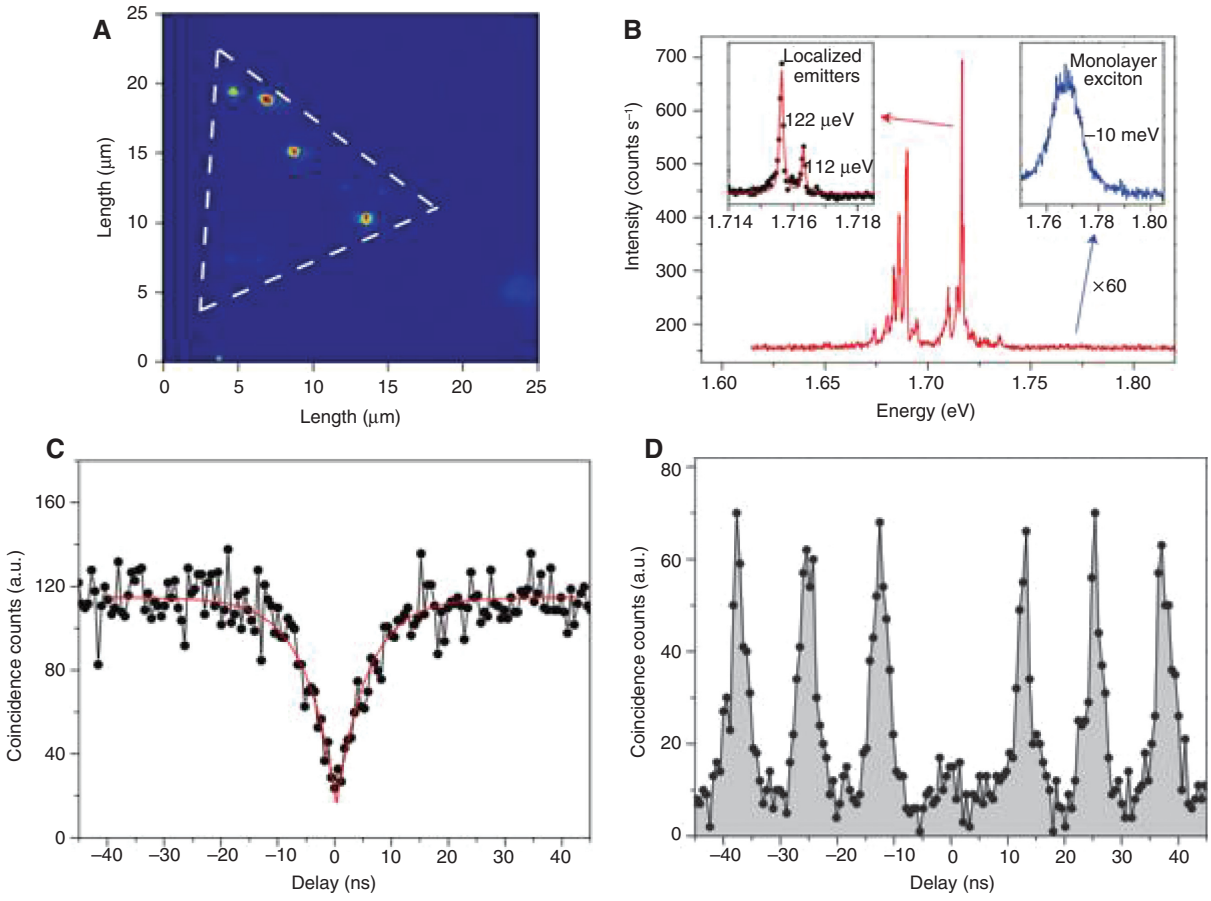

Figure 9: Single quantum emitters in layered materials.
(A) Photoluminescence intensity map of narrow emission lines over 25 μm × 25 μm area. The dashed triangle indicates the position of the monolayer; (B) photoluminescence spectrum of localized emitters. The left inset is a high-resolution spectrum of a defect emission. The right inset is a zoom-in of the monolayer valley exciton emission; observation of photon anti-bunching with (C) CW and (D) pulsed excitation. The dip at zero time-delay indicates presence of single photons. This figure is reprinted from Ref. [111].

photon nonlinear optics using the off-resonant nonlinearity. However, the quality factor needed to reach the single photon nonlinear optical regime is generally very high, ~10^5–10^6, and it is not yet clear whether such a high Q can be reached with a polymer-based transfer process of layered materials. The creation of the quantum dot like structures by lithography is promising, but the effect of etching on the non-radiative excitonic decay rate is not clear.

A more straightforward route would be to exploit quantum emitters in layered materials. Recently several research groups have reported single quantum emitters in layered materials, particularly in TMDCs and in h-BN [111–114]. These single emitters originate from the localized defects in the crystals [115]. Figure 9A shows the scanning PL data from a chemical vapor deposition-grown WSe_2 flake, where the bright defects can be clearly identified. When such a bright spot is spatially separated, the measured spectrum shows narrow lines, indicative of single defects (Figure 9B). Via second-order autocorrelation measurements under both CW and pulsed excitation (Figure 9C and D), a $g^{(2)}(0) < 0.5$ is measured, which unambiguously proves single photon emission from these defects. Via coupling two-level quantum emitters, such as quantum dots, with an optical cavity, strong nonlinear optical effects, such as single photon switching [116–118] and photon blockade [119–121] have been observed. A similar performance is expected from the defects in layered materials as well. To this end, Tran et al. [122] have coupled the single defects in h-BN to plasmonic resonators. The plasmonic pillars enhanced the overall brightness of the emitters by a factor of two. These emitters are also recently excited by two-photon processes [123]. Recently, enhancement of the quantum emitters in WSe_2 was also observed using silver nanowires, where the emission was coupled to a surface plasmon polariton mode [124]. Finally, very recently, scalable growth of defects in layered material has been demonstrated [125]. In this work, monolayers of WSe_2 and WS_2 were transferred in a templated vertical silica nano-pillar, and with high probability the defects were localized near the pillar. The wavelength of the defect emission also can be controlled by the pillar diameter. Such capability of deterministic positioning and wavelength selection can solve the long-standing problem of stochastic positioning and large inhomogeneous broadening of quantum dots, which have largely limited the scalable operation of quantum dots, and other quantum emitters. The defects in layered materials thus can provide a scalable platform of single photon nonlinear devices.

8 Outlook

The field of the cavity nonlinear optics with layered materials is in its infancy. The majority of researchers working with layered materials still primarily focus on the spectroscopy and material characterization, and the effort on integration with nanophotonic resonant structures is relatively recent. However, the unprecedented material compatibility, easy availability of the materials, and unique optoelectronic properties of the layered materials have very quickly generated strong interest in the nanophotonics community. Hence, we are hopeful that integration of layered materials with nanophotonic devices will enable more fundamentally new scientific studies, and novel low-power applications in the near future. As explained earlier, all the reported nonlinearities can be enhanced by improving the cavities (larger Q and smaller V), and this will surely drive future research on cavity nonlinear optics with layered material systems. In this section, we elaborate on some of the new and more speculative research directions involving cavity nonlinear optics with layered materials.

8.1 Phase transition layered materials

Phase transition in layered materials, such as $MoTe_2$ and WTe_2 has been predicted [126–128]. Bulk phase change materials, such as GeSbTe (GST), have recently generated a lot of interest in the field of integrated nanophotonics due to the large change in the refractive index associated with the structural change in GST [129–131]. Coupled with an optical resonator, such large change in refractive index will enable optical bistability, where the output optical power is a strongly nonlinear function of the input optical power. One major problem of GST, however, is the large amount of loss in the visible and near-infrared frequency. The layered phase change materials have a wider band gap, and can provide a new way to realize a very large change in the refractive indices, while maintaining a low loss.

8.2 Heterostructure of layered materials

Several groups have reported fabrication and characterization of heterostructures of layered materials [132, 133]. One particularly interesting aspect of the heterostructure is the observation of long-lived inter-layer excitons, where the electron and holes are separated into different layers. This prevents the recombination of the electron and hole

pair, and thus long-lived exciton states can be realized. The implication of such long-lived excitons for nonlinear optics is not clear, and can potentially constitute a new research field. For example, what are the implications for exciton-polaritons and exciton-polaritons BEC with long-lived excitons? Furthermore, by separating different TMDC layers by h-BN, a multi-quantum well-like structure can be realized, where the thickness of the nonlinear material can be varied. Researchers have already demonstrated stronger exciton-photon coupling in bilayer $MoSe_2$ separated by h-BN [35]. With N layers, we expect the coupling strength to increase by a factor of $\sqrt{N}$.

8.3 Valley exciton-polaritons

TMDCs exhibit unique spin-valley physics, which primarily stems from the combination of two features. First, the band gap is at the $+K$ and $-K$ "Dirac valleys", not at the Brillouin zone center. This gives the electron states a "valley index" (or pseudospin) in addition to real spin [134, 135]. Optical selection rules are such that right hand circularly polarized light (σ^+) couples only to one valley and left hand circularly polarized light (σ^-) couples to the other, providing the first solid-state system in which dynamic control of valley pseudospin is possible [134, 136–142]. Second, the strong spin-orbit coupling locks the real spin at the band edges to the valley index [134]. Spontaneous transitions between these spin-states are unlikely due to the large mismatch between momentum vectors. Several research groups have observed valley physics in the exciton-polariton system [143–145]. Surprisingly, the results show that the hybridization with cavity photons makes it easier to observe the spin-valley physics at room temperature [143], and for materials, where the exciton does not ordinarily demonstrate strong spin-valley physics [145]. However, the spin-valley physics remained largely ignored in the cavity nonlinear optics with monolayer materials. In III-V quantum well systems, researchers demonstrated a helicity dependent polariton-polariton interaction. Exploiting such an effect, multistability in helicity is observed in exciton-polariton systems [146, 147]. Similar effects are expected with TMDC exciton-polaritons as well. The multistable devices can enable multi-state optical logic.

8.4 Hyperbolic metamaterial with layered materials

In all the nonlinear systems we have considered in this article so far, the layered materials only provide the required nonlinearity and the cavity is formed by another, linear material. However, it is possible to fabricate a whole photonic structure using layered materials. For example, using graphene and h-BN layered structures, researchers predicted that a hyperbolic metamaterial can be created [148, 149]. Hyperbolic metamaterials are promising candidates for enhancing the nonlinear optical interaction [150]. Thus, it is possible to build a nonlinear nanophotonic system solely made out of layered materials. This will open a completely new field of research.

Acknowledgments: The authors acknowledge useful discussion with Professor Vinod Menon, Professor Xiaodong Xu and Professor Feng Wang. This work is supported by the National Science Foundation under grant NSF-EFRI-1433496, and the Air Force Office of Scientific Research-Young Investigator Program under grant FA9550-15-1-0150.

References

[1] Xia F, Wang H, Xiao D, Dubey M, Ramasubramaniam A. Two-dimensional material nanophotonics. Nat Photonics 2014;8:899–907.
[2] Xi X, Wang Z, Zhao W, et al. Ising pairing in superconducting NbSe2 atomic layers. Nat Phys 2016;12:139–43.
[3] Navarro-Moratalla E, Island JO, Mañas-Valero S, et al. Enhanced superconductivity in atomically thin TaS2. 2016;7:11043.
[4] Liu F, You L, Seyler KL, et al. Room-temperature ferroelectricity in CuInP2S6 ultrathin flakes. 2016;7:12357.
[5] Je-Geun P. Opportunities and challenges of 2D magnetic van der Waals materials: magnetic graphene? J Phys: Condens Matter 2016;28:301001.
[6] Gong C, Li L, Li Z, et al. Discovery of intrinsic ferromagnetism in two-dimensional van der Waals crystals. Nature 2017;546:265–9.
[7] Huang B, Clark G, Navarro-Moratalla E, et al. Layer-dependent ferromagnetism in a van der Waals crystal down to the monolayer limit. Nature 2017;546:270–3.
[8] Malard LM, Alencar TV, Barboza APM, Mak KF, de Paula AM. Observation of intense second harmonic generation from MoS_2 atomic crystals. Phys Rev B 2013;87:201401.
[9] Hochberg M, Baehr-Jones T. Towards fabless silicon photonics. Nat Photonics 2010;4:492–4.
[10] Geim AK, Novoselov KS. The rise of graphene. Nat Mater 2007;6:183–91.
[11] Schwierz F. Graphene transistors. Nat Nanotechnol 2010;5:487–96.
[12] Wang H, Hsu A, Wu J, Kong J, Palacios T. Graphene-based ambipolar RF mixers. IEEE Electron Device Lett 2010;31:906–8.
[13] Schedin F, Geim AK, Morozov SV, et al. Detection of individual gas molecules adsorbed on graphene. Nat Mater 2007;6:652–5.
[14] Wang F, Zhang Y, Tian C, et al. Gate-variable optical transitions in graphene. Science 2008;320:206–9.

[15] Fei Z, Rodin AS, Andreev GO, et al. Gate-tuning of graphene plasmons revealed by infrared nano-imaging. Nature 2012;487:82–5.
[16] Nair RR, Blake P, Grigorenko AN, et al. Fine structure constant defines visual transparency of graphene. Science 2008;320:1308.
[17] Liu M, Yin X, Ulin-Avila E, et al. A graphene-based broadband optical modulator. Nature 2011;474:64–7.
[18] Phare CT, Daniel Lee YH, Cardenas J, Lipson M. Graphene electro-optic modulator with 30 GHz bandwidth. Nat Photonics 2015;9:511–4.
[19] Gan X, Shiue R-J, Gao Y, et al. Chip-integrated ultrafast graphene photodetector with high responsivity. Nat Photonics 2013;7:883–7.
[20] Mueller T, Xia F, Avouris P. Graphene photodetectors for high-speed optical communications. Nat Photonics 2010;4:297–301.
[21] Xia F, Mueller T, Lin Y-M, Valdes-Garcia A, Avouris P. Ultrafast graphene photodetector. Nat Nanotechnol 2009;4:839–43.
[22] Gan X, Shiue R-J, Gao Y, et al. High-contrast electrooptic modulation of a photonic crystal nanocavity by electrical gating of graphene. Nano Lett 2013;13:691–6.
[23] Majumdar A, Kim J, Vuckovic J, Wang F. Electrical control of silicon photonic crystal cavity by graphene. Nano Lett 2013;13:515–8.
[24] Wei W, Nong J, Zhu Y, et al. Cavity-enhanced continuous graphene plasmonic resonator for infrared sensing. Opt Commun 2017;395:147–53.
[25] Kim J, Son H, Cho DJ, et al. Electrical control of optical plasmon resonance with graphene. Nano Lett 2012;12:5598–602.
[26] Majumdar A, Jonghwan K, Vuckovic J, Feng W. Graphene for tunable nanophotonic resonators. IEEE J Sel Top Quantum Electron 2014;20:68–71.
[27] Vahala KJ. Optical microcavities. Nature 2003;424:839–46.
[28] Gan X, Gao Y, Fai Mak K, et al. Controlling the spontaneous emission rate of monolayer MoS_2 in a photonic crystal nanocavity. Appl Phys Lett 2013;103:181119.
[29] Wu S, Buckley S, Jones AM, et al. Control of two-dimensional excitonic light emission via photonic crystal. 2D Mater 2014;1011001.
[30] Wei G, Stanev T, Stern N, Czaplewski D, Jung W. Interfacing monolayer MoS_2 with silicon-nitride integrated photonics. In Advanced Photonics, Boston, Massachusetts, 2015, p. IM4A.3.
[31] Wu S, Buckley S, Schaibley JR, et al. Monolayer semiconductor nanocavity lasers with ultralow thresholds. Nature 2015;520:69–72.
[32] Ye Y, Wong ZJ, Lu X, et al. Monolayer excitonic laser. Nat Photonics 2015;9:733–7.
[33] Salehzadeh O, Djavid M, Tran NH, Shih I, Mi Z. Optically pumped two-dimensional MoS_2 lasers operating at room-temperature. Nano Lett 2015;15:5302–6.
[34] Liu CH, Clark G, Fryett T, et al. Nanocavity integrated van der Waals heterostructure light-emitting tunneling diode. Nano Lett 2017;17:200–5.
[35] Dufferwiel S, Schwarz S, Withers F, et al. Exciton-polaritons in van der Waals heterostructures embedded in tunable microcavities. Nat Commun 2015;6:8579.
[36] Liu X, Galfsky T, Sun Z, et al. Strong light-matter coupling in two-dimensional atomic crystals. Nat Photonics 2015;9:30–4.
[37] Liu K, Sun S, Majumdar A, Sorger VJ. Fundamental scaling laws in nanophotonics. Sci Rep 2016;6:37419.
[38] Trivedi R, Khankhoje UK, Majumdar A. Cavity-enhanced second-order nonlinear photonic logic circuits. Phys Rev Appl 2016;5:054001.
[39] Hong S-Y, Dadap JI, Petrone N, Yeh P-C, Hone J, Osgood RM. Optical third-harmonic generation in graphene. Phys Rev X 2013;3:021014.
[40] Cheng JL, Vermeulen N, Sipe JE. Third order optical nonlinearity of graphene. New J Phys 2014;16:053014.
[41] Youngblood N, Peng R, Nemilentsau A, Low T, Li M. Layer-tunable third-harmonic generation in multilayer black phosphorus. ACS Photonics 2017;4:8–14.
[42] Woodward RI, Murray RT, Phelan CF, et al. Characterization of the second- and third-order nonlinear optical susceptibilities of monolayer MoS_2 using multiphoton microscopy. 2D Mater 2017;4:011006.
[43] Karvonen L, Säynätjoki A, Mehravar S, et al. Investigation of second- and third-harmonic generation in few-layer gallium selenide by multiphoton microscopy. Sci Rep 2015;5:10334.
[44] Cui Q, Muniz RA, Sipe JE, Zhao H. Strong and anisotropic third-harmonic generation in monolayer and multilayer ReS_2. Phys Rev B 2017;95:165406.
[45] Seyler KL, Schaibley JR, Gong P, et al. Electrical control of second-harmonic generation in a WSe_2 monolayer transistor. Nat Nano 2015;10:407–11.
[46] Janisch C, Wang Y, Ma D, et al. Extraordinary second harmonic generation in tungsten disulfide monolayers. Sci Rep 2014;4.
[47] Kumar N, Najmaei S, Cui Q, et al. Second harmonic microscopy of monolayer MoS_2. Phys Rev B 2013;87:161403.
[48] Ribeiro-Soares J, Janisch C, Liu Z, et al. Second harmonic generation in WSe 2. 2D Mater 2015;2:045015.
[49] Li Y, Rao Y, Mak KF, et al. Probing symmetry properties of few-layer MoS_2 and h-BN by optical second-harmonic generation. Nano Lett 2013;13:3329–33.
[50] Zhou X, Cheng J, Zhou Y, et al. Strong second-harmonic generation in atomic layered GaSe. J Am Chem Soc 2015;137:7994–7.
[51] Zeng H, Liu G-B, Dai K, et al. Optical signature of symmetry variations and spin-valley coupling in atomically thin tungsten dichalcogenides. Sci Rep 2013;3.
[52] Yin X, Ye Z, Chenet DA, et al. Edge nonlinear optics on a MoS_2 atomic monolayer. Science 2014;344:488–90.
[53] Hsu W-T, Zhao Z-A, Li L-J, et al. Second harmonic generation from artificially stacked transition metal dichalcogenide twisted bilayers. ACS Nano 2014;8:2951–8.
[54] Heo H, Sung JH, Cha S, et al. Interlayer orientation-dependent light absorption and emission in monolayer semiconductor stacks. Nat Commun 2015;6:7372.
[55] Klein J, Wierzbowski J, Steinhoff A, et al. Electric-field switchable second-harmonic generation in bilayer MoS_2 by inversion symmetry breaking. Nano Lett 2017;17:392–8.
[56] Conley HJ, Wang B, Ziegler JI, Haglund RF, Pantelides ST, Bolotin KI. Bandgap engineering of strained monolayer and bilayer MoS_2. Nano Lett 2013;13:3626–30.
[57] Castellanos-Gomez A, Roldán R, Cappelluti E, et al. Local strain engineering in atomically thin MoS_2. Nano Lett 2013;13:5361–6.
[58] Zhu CR, Wang G, Liu BL, et al. Strain tuning of optical emission energy and polarization in monolayer and bilayer MoS_2. Phy Rev B 2013;88:121301.

[59] Trolle ML, Seifert G, Pedersen TG. Theory of excitonic second-harmonic generation in monolayer MoS_2. Phys Rev B 2014;89:235410.
[60] Grüning M, Attaccalite C. Second harmonic generation in *h*-BN and MoS_2 monolayers: role of electron-hole interaction. Phys Rev B 2014;89:081102.
[61] Wang CY, Guo G-Y. Nonlinear optical properties of transition-metal dichalcogenide MX2 (M=Mo, W; X=S, Se) monolayers and trilayers from first-principles calculations. J Phys Chem C 2015;119:13268–76.
[62] Merano M. Nonlinear optical response of a two-dimensional atomic crystal. Opt Lett 2016;41:187–90.
[63] Fryett T, Dodson CM, Majumdar A. cavity enhanced nonlinear optics for few photon optical bistability. Opt Express 2015;23:16246–55.
[64] Smirnova DA, Solntsev AS. Cascaded third-harmonic generation in hybrid graphene-semiconductor waveguides. Phys Rev B 2015;92:155410.
[65] Hendry E, Hale PJ, Moger J, Savchenko AK, Mikhailov SA. Coherent nonlinear optical response of graphene. Phys Rev Lett 2010;105:097401.
[66] Wang G, Zhang S, Zhang X, et al. Tunable nonlinear refractive index of two-dimensional MoS_2, WS2, and MoSe2 nanosheet dispersions [Invited], Photon Res 2015;3:A51–5.
[67] Khurgin J-B. Graphene – A rather ordinary nonlinear optical material. Appl Phys Lett 2014;104:161116.
[68] Majumdar A, Dodson CM, Fryett TK, Zhan A, Buckley S, Gerace D. Hybrid 2D material nanophotonics: a scalable platform for low-power nonlinear and quantum optics. ACS Photon 2015;2:1160–6.
[69] Boyd RW. Nonlinear Optics. Third ed., Academic Press.
[70] Lin Z, Liang X, Lončar M, Johnson SG, Rodriguez AW. Cavity-enhanced second-harmonic generation via nonlinear-overlap optimization. Optica 2016;3:233–8.
[71] Fryett TK, Zhan A, Majumdar A. Phase matched nonlinear optics via patterning layered materials. Opt Lett 2017;42:3586–9.
[72] Li X, Zhu J, Wei B. Hybrid nanostructures of metal/two-dimensional nanomaterials for plasmon-enhanced applications. Chem Soc Rev 2016;45:3145–87.
[73] Akselrod GM, Ming T, Argyropoulos C, et al. Leveraging nanocavity harmonics for control of optical processes in 2D semiconductors. Nano Lett 2015;15:3578–84.
[74] Chen C, Youngblood N, Peng R, et al. Three-dimensional integration of black phosphorus photodetector with silicon photonics and nanoplasmonics. Nano Lett 2017;17:985–91.
[75] Lee B, Liu W, Naylor CH, et al. Electrical tuning of exciton–plasmon polariton coupling in monolayer MoS_2 integrated with plasmonic nanoantenna lattice. Nano Lett 2017;17:4541–7.
[76] Fryett TK, Seyler KL, Zheng J, Liu C-H, Xu X, Majumdar A. Silicon photonic crystal cavity enhanced second-harmonic generation from monolayer WSe_2. 2D Mater 2016;4.
[77] Day JK, Chung M-H, Lee Y-H, Menon VM. Microcavity enhanced second harmonic generation in 2D MoS_2. Opt Mater Express 2016;6:2360–5.
[78] Hammer S, Mangold HM, Nguyen AE, et al. Scalable and transfer-free fabrication of MoS_2/SiO2 hybrid nanophotonic cavity arrays with quality factors exceeding 4000. Sci Rep 2017;7:7251.
[79] Gan X, Zhao C, Hu S, et al. Microwatts continuous-wave pumped second harmonic generation in few- and mono-layer GaSe. 2017;arXiv:1706.07923.
[80] Dolan PR, Hughes GM, Grazioso F, Patton BR, Smith JM. Femtoliter tunable optical cavity arrays. Opt Lett 2010;35:3556–8.
[81] Yi F, Ren M, Reed JC, et al. Optomechanical enhancement of doubly resonant 2D optical nonlinearity. Nano Lett 2016;16:1631–6.
[82] Chen H, Corboliou V, Solntsev AS, et al. Enhanced second-harmonic generation from two-dimensional MoSe2 by waveguide integration. In Conference on Lasers and Electro-Optics, San Jose, California, 2017, p. FM2F.4.
[83] Guo X, Zou C-L, Jung H, Tang HX. On-chip strong coupling and efficient frequency conversion between telecom and visible optical modes. Phys Rev Lett 2016;117:123902.
[84] Wang H, Qian X. Giant optical second harmonic generation in two-dimensional multiferroics. Nano Lett 2017;17:5027–34.
[85] Gu T, Petrone N, McMillan JF, et al. Regenerative oscillation and four-wave mixing in graphene optoelectronics. Nat Photonics 2012;6:554–9.
[86] Pernice WHP, Li M, Gallagher DFG, Tang HX. Silicon nitride membrane photonics. J Opt A: Pure Appl Opt 2009;11:114017.
[87] Ikeda K, Saperstein RE, Alic N, Fainman Y. Thermal and Kerr nonlinear properties of plasma-deposited silicon nitride/silicon dioxide waveguides. Opt Express 2008;16:12987–94.
[88] Ma J, Xie GQ, Lv P, et al. Graphene mode-locked femtosecond laser at 2 micron wavelength. Opt Lett 2012;37:2085–7.
[89] Sun Z, Hasan T, Torrisi F, et al. Graphene mode-locked ultrafast laser. ACS Nano 2010;4:803–10.
[90] Bao Q, Zhang H, Wang Y, et al. Atomic-layer graphene as a saturable absorber for ultrafast pulsed lasers. Adv Funct Mater 2009;19:3077–83.
[91] Chen Y, Jiang G, Chen S, et al. Mechanically exfoliated black phosphorus as a new saturable absorber for both Q-switching and mode-locking laser operation. Opt Express 2015;23:12823–33.
[92] Aiub EJ, Steinberg D, Thoroh de Souza EA, Saito LAM. 200-fs mode-locked Erbium-doped fiber laser by using mechanically exfoliated MoS_2 saturable absorber onto D-shaped optical fiber. Opt Express 2017;25:10546–52.
[93] Mao D, Wang Y, Ma C, et al. WS2 mode-locked ultrafast fiber laser. Sci Rep 2015;5:7965.
[94] Liu H, Sun Z, Wang X, Wang Y, Cheng G. Several nanosecond Nd:YVO4 lasers Q-switched by two dimensional materials: tungsten disulfide, molybdenum disulfide, and black phosphorous. Opt Express 2017;25:6244–52.
[95] Carusotto I, Ciuti C. Quantum fluids of light. Rev Mod Phys 2013;85:299–366.
[96] Byrnes T, Kim NY, Yamamoto Y. Exciton-polariton condensates. Nat Phys 2014;10:803–13.
[97] Deng H, Haug H, Yamamoto Y. Exciton-polariton Bose-Einstein condensation. Rev Mod Phys 2010;82:1489–537.
[98] Jiang J-H, John S. Photonic architectures for equilibrium high-temperature Bose-Einstein condensation in dichalcogenide monolayers. Sci Rep 2014;4:7432.
[99] Karzig T, Bardyn C-E, Lindner NH, Refael G. Topological polaritons. Phys Rev X 2015;5:031001.

[100] Cotleţ O, Zeytinoğlu S, Sigrist M, Demler E, Imamoğlu A. Superconductivity and other collective phenomena in a hybrid Bose-Fermi mixture formed by a polariton condensate and an electron system in two dimensions. Phys Rev B 2016;93:054510.
[101] Wei G, Czaplewski DA, Lenferink EJ, Stanev TK, Jung IW, Stern NP. Size-tunable Lateral Confinement in Monolayer Semiconductors. Scientific Reports 2017; 7: Article number: 3324. doi:10.1038/s41598-017-03594-z
[102] Verger A, Ciuti C, Carusotto I. Polariton quantum blockade in a photonic dot. Phys Rev B 2006;73:193306.
[103] Wang H-X, Zhan A, Xu Y-D, et al. Quantum many-body simulation using monolayer exciton-polaritons in coupled-cavities. J Phys: Condensed Matter 2017:29. DOI: 10.1088/1361-648X/aa8933.
[104] Majumdar A, Rundquist A, Bajcsy M, Dasika VD, Bank SR, Vučković J. Design and analysis of photonic crystal coupled cavity arrays for quantum simulation. Phys Review B 2012;86:195312.
[105] Altug H, Englund D, Vuckovic J. Ultrafast photonic crystal nanocavity laser. Nat Phys 2006;2:484–8.
[106] Eisert J, Friesdorf M, Gogolin C. Quantum many-body systems out of equilibrium. Nat Phys 2015;11:124–30.
[107] Changsuk N, Dimitris GA. Quantum simulations and many-body physics with light. Rep Prog Phys 2017;80:016401.
[108] Michael JH. Quantum simulation with interacting photons. J Opt 2016;18:104005.
[109] Ferretti S, Gerace D. Single-photon nonlinear optics with Kerr-type nanostructured materials. Phys Rev B 2012;85:033303.
[110] Majumdar A, Gerace D. Single-photon blockade in doubly resonant nanocavities with second-order nonlinearity. Phys Rev B 2013;87:235319.
[111] He Y-M, Clark G, Schaibley JR, et al. Single quantum emitters in monolayer semiconductors. Nat Nanotechnol 2015;10: 497–502.
[112] Koperski M, Nogajewski K, Arora A, et al. Single photon emitters in exfoliated WSe_2 structures. Nat Nano 2015;10:503–6.
[113] Srivastava A, Sidler M, Allain AV, Lembke DS, Kis A, Imamoğlu A. Optically active quantum dots in monolayer WSe_2. Nat Nano 2015;10:491–6.
[114] Tran TT, Bray K, Ford MJ, Toth M, Aharonovich I. Quantum emission from hexagonal boron nitride monolayers. Nat Nano 2016;11:37–41.
[115] Zhong L, Bruno RC, Ethan K, et al. Defect engineering of two-dimensional transition metal dichalcogenides. 2D Mater 2016;3:022002.
[116] Englund D, Majumdar A, Bajcsy M, Faraon A, Petroff P, Vučković J. Ultrafast photon-photon interaction in a strongly coupled quantum dot-cavity system. Phys Rev Lett 2012;108:093604.
[117] Bose R, Sridharan D, Kim H, Solomon GS, Waks E. Low-photon-number optical switching with a single quantum dot coupled to a photonic crystal cavity. Phys Rev Lett 2012;108:227402.
[118] Volz T, Reinhard A, Winger M, et al. Ultrafast all-optical switching by single photons. Nat Photonics 2012;6:605–9.
[119] Faraon A, Fushman I, Englund D, Stoltz N, Petroff P, Vuckovic J. Coherent generation of non-classical light on a chip via photon-induced tunnelling and blockade. Nat Phys 2008;4:859–63.
[120] Majumdar A, Bajcsy M, Vučković J. Probing the ladder of dressed states and nonclassical light generation in quantum-dot–cavity QED. Phys Rev A 2012;85:041801.
[121] Reinhard A, Volz T, Winger M, et al. Strongly correlated photons on a chip. Nat Photonics 2012;6:93–6.
[122] Tran TT, Wang D, Xu ZQ, et al. Deterministic coupling of quantum emitters in 2D materials to plasmonic nanocavity arrays. Nano Lett 2017;17:2634–9.
[123] Schell AW, Tran TT, Takashima H, Takeuchi S, Aharonovich I. Non-linear excitation of quantum emitters in hexagonal boron nitride multiplayers. APL Photonics 2016;1:091302.
[124] Cai T, Dutta S, Aghaeimeibodi S, et al. Coupling emission from single localized defects in 2D semiconductor to surface plasmon polaritons. Nano Lett 2017;17:6564–8. DOI: 10.1021/acs.nanolett.7b02222.
[125] Palacios-Berraquero C, Kara DM, Montblanch ARP, et al. Large-scale quantum-emitter arrays in atomically thin semiconductors. Nat Commun 2017;8:15093.
[126] Li Y, Duerloo K-AN, Wauson K, Reed EJ. Structural semiconductor-to-semimetal phase transition in two-dimensional materials induced by electrostatic gating. Nat Commun 2016;7:10671.
[127] Duerloo K-AN, Li Y, Reed EJ. Structural phase transitions in two-dimensional Mo- and W-dichalcogenide monolayers. Nat Commun 2014;5:4214.
[128] Duerloo K-AN, Reed EJ. Structural phase transitions by design in monolayer alloys. ACS Nano 2016;10:289–97.
[129] Ríos A, Stegmaier M, Hosseini P, et al. Integrated all-photonic non-volatile multi-level memory. Nat Photonics 2015;9:725–32.
[130] Liang H, Soref R, Mu J, Majumdar A, Li X, Huang W-P. Simulations of silicon-on-insulator channel-waveguide electrooptical 2x2 switches and 1x1 modulators using a GeSeTe self-holding layer. J Lightwave Technol 2015;33:1805–13.
[131] Hosseini P, Wright CD, Bhaskaran H. An optoelectronic framework enabled by low-dimensional phase-change films. Nature 2014;511:206–11.
[132] Geim A, Grigorieva I. Van der Waals heterostructures. Nature 2013;499:419–25.
[133] Rivera P, Schaibley JR, Jones AM, et al. Observation of long-lived interlayer excitons in monolayer MoSe2–WSe_2 heterostructures. Nat Commun 2015;6.
[134] Xiao D, Liu G-B, Feng W, Xu X, Yao W. Coupled spin and valley physics in monolayers of MoS_2 and other group-VI dichalcogenides. Phys Rev Lett 2012;108:196802.
[135] Xu X, Yao W, Xiao D, Heinz TF. Spin and pseudospins in layered transition metal dichalcogenides. Nat Phys 2014;10:343–50.
[136] Cao T, Wang G, Han W, et al. Valley-selective circular dichroism of monolayer molybdenum disulphide. Nat Commun 2012;3:2012.
[137] Zeng H, Dai J, Yao W, Xiao D, Cui AX. Valley polarization in MoS_2 monolayers by optical pumping. Nat Nanotechnol 2012;7:490–3.
[138] Jones AM, Yu H, Ghimire NJ, et al. Optical generation of excitonic valley coherence in monolayer WSe_2. Nat Nanotechnol 2013;8:634–8.
[139] Mak KF, He K, Shan J, Heinz TF. Control of valley polarization in monolayer MoS_2 by optical helicity. Nat Nanotechnol 2012;7:494–8.
[140] Li Y. Valley splitting and polarization by the Zeeman effect in monolayer MoSe2. In: Probing the response of two-dimensional crystals by optical spectroscopy. Springer Theses (Recognizing Outstanding Ph.D. Research). Springer: Cham, 2016. DOI: https://doi.org/10.1007/978-3-319-25376-3_7.

[141] Srivastava A, Sidler M, Allain AV, Lembke DS, Kis A, Imamoglu A. Valley Zeeman effect in elementary optical excitations of a monolayer WSe_2. Nature Physics 2015;11:141–7. doi:10.1038/nphys3203.
[142] Bajoni D, Senellart P, Wertz E, et al. Polariton laser using single micropillar GaAs-GaAlAs semiconductor cavities. Phys Rev Lett 208;100:047401.
[143] Chen Y-J, Cain JD, Stanev TK, Dravid VP, Stern NP. Valley-polarized exciton–polaritons in a monolayer semiconductor. Nat Photonics 2017;11:431–5.
[144] Sun Z, Gu J, Ghazaryan A, et al. Optical control of room-temperature valley polaritons. Nat Photonics 2017;11:491–6.
[145] Dufferwiel S, Lyons TP, Solnyshkov DD, et al. Valley-addressable polaritons in atomically thin semiconductors. Nat Photonics 2017;11:497–501.
[146] Paraïso TK, Wouters M, Léger Y, Morier-Genoud F, Deveaud-Plédran B. Multistability of a coherent spin ensemble in a semiconductor microcavity. Nat Mater 2010;9:655–60.
[147] Gippius NA, Shelykh IA, Solnyshkov DD, et al. Polarization multistability of cavity polaritons. Phys Rev Lett 2007;98:236401.
[148] Dai S, Ma Q, Liu MK, et al. Graphene on hexagonal boron nitride as a tunable hyperbolic metamaterial. Nat Nanotechnol 2015;10:682–6.
[149] Kumar A, Low T, Fung KH, Avouris P, Fang NX. Tunable light–matter interaction and the role of hyperbolicity in graphene–hBN system. Nano Lett 2015;15:3172–80.
[150] Poddubny A, Iorsh I, Belov P, Kivshar Y. Hyperbolic metamaterials. Nat Photonics 2013;7:948–57.